Quasi-dynamical electron diffraction – a kinematic type of expression for the dynamical diffracted-beam amplitudes

Lian-Mao Peng

Beijing Laboratory of Electron Micoscopy, Center for Condensed Matter Physics and Institute of Physics, Chinese Academy of Sciences, PO Box 2724, Beijing 100080, People's Republic of China, and Department of Electronics, Peking University, Beijing 100871, People's Republic of China. Correspondence e-mail: lmpeng@lmplab.blem.ac.cn

It is shown that to a good approximation the dynamical diffracted electron-beam amplitudes may be expressed in a form that is identical to that of the kinematic theory of electron diffraction. The validity of this approximate form of the dynamical electron diffraction is illustrated for thin films of GaAs and Au crystals, and its implications in electron crystallography for structural determination and refinement are discussed.

1. Introduction

In recent years, the field of electron crystallography has been becoming increasingly active as more and more experimental evidence has emerged pointing toward the usefulness of the kinematic type of approaches for dealing with electron diffraction data (see Vincent *et al.*, 1984; Li & Tang, 1985; Gjønnes *et al.*, 1989; Peng & Wang, 1994; Dorset, 1995; Van Dyck & Op de Beeck, 1996; Marks & Landree, 1998) and many articles in Tivol (1999). The kinematic theory of electron diffraction is based on two approximations. Firstly, it assumes that the total electrostatic potential of a crystal may be expressed as a summation over contributions of individual atoms

$$V(\mathbf{r}) = \sum_n \phi(\mathbf{r} - \mathbf{r}_n),$$

where $\phi_n(\mathbf{r})$ is the electrostatic potential associated with the nth atoms. In making this partition, we have neglected charge redistribution in the crystals. This is nevertheless an excellent approximation, which is accurate for all but the lowest-order reflections, and even for these lowest-order reflections the error introduced by using this approximation is typically no more than 2 to 5% (Spence, 1993; Ren *et al.*, 1997). For almost all structural electron crystallography work, the accuracy is not limited by the use of this approximation.

The second approximation used in the kinematic theory is more severe, which assumes that the diffracted electron-beam amplitude equals the Fourier transform of the total electrostatic potential,

$$A(\mathbf{g}) = \mathcal{F}\{V(\mathbf{r})\} = \sum_n f_n(s) \exp(2\pi i \mathbf{g} \cdot \mathbf{r}_n), \qquad (1)$$

with $s = g/2$ and $f(s) = \mathcal{F}\{\phi(\mathbf{r})\}$ being the usual *electron atomic scattering factor* (Cowley, 1992). We note here that the electron atomic scattering factor defined in this way is in general a real quantity. The usefulness of the kinematic formulation lies in the facts that the diffracted-beam amplitude may be evaluated readily *via* a simple summation operation, rather than the much more complicated matrix diagonalization [as in the Bloch-wave-based theories of dynamical electron diffraction (Hirsch *et al.*, 1977; Humphreys, 1979; Spence & Zuo, 1992)] or multiple Fourier transforms in both the real and reciprocal space [as in the multislice method of Cowley & Moodie (Cowley & Moodie, 1957; Goodman & Moodie, 1974)], and that many efficient crystallographic methods developed in X-ray diffraction for structural determination and refinement may be used directly (Woolfson & Fan, 1995). It is, however, a well established fact that electron diffraction by a crystal is dominated by multiple-scattering events (Glauber & Schomaker, 1953; Hoerni & Ibers, 1953; Ibers & Hoerni, 1954; Cowley, 1990; Peng & Wang, 1994), and that the kinematic theory of electron diffraction cannot be used quantitatively even for a monolayer of atoms. To illustrate the dynamical nature of electron diffraction, we have shown in Fig. 1 plots of the phase and amplitude of the scattered 100 keV electron as a function of $s = \sin\theta/\lambda$, with θ being the half angle of scattering and λ the wavelength of the incident electron. The figure shows clearly that the phase depends on the angle of scattering, which is in contrast to the ideal kinematic case of electron diffraction where the phase equals zero for all angles of scattering. In this article, we will present a simple kinematic type of expression for the dynamical diffracted-electron-beam amplitudes and show that this expression may account well for the magnitude and phase

variations with angles of scattering for thin films composed of almost all types of atoms.

2. Phase-object approximation and quasi-dynamical theory

We start our discussions from a very powerful approximation widely used in high-resolution imaging of atomic structures of crystals, that is the *phase-object approximation* (POA) [first introduced in Section 7(*a*) of Cowley & Moodie (1957)]. This approximation is valid for thin crystals composed of all types of atoms, including heavy atoms, and it becomes less accurate for crystals that are thicker than say 10 nm. Using this approximation, we may write the exit electron wave function on the bottom face of a thin crystal as

$$\psi(\mathbf{x}) = \exp\left\{i \sum_n \varphi_n(\mathbf{x} - \mathbf{x}_n)\right\},$$

where $\varphi_n(\mathbf{x})$ denotes the projected atomic potential for the *n*th atom along the beam direction:

$$\varphi(\mathbf{x}) = \sigma \int \phi(\mathbf{x}, z) \, dz,$$

where $\sigma = 2\pi me\lambda/\hbar^2$ is the relativistic electron interaction constant (Cowley, 1990). The diffracted-beam amplitude $A(\mathbf{q})$ is then given by a Fourier transform of the exit electron wave function

$$\begin{aligned} A(\mathbf{q}) &= \mathcal{F}\{\psi(\mathbf{x})\} \\ &= \mathcal{F}\{\exp[i\varphi_1(\mathbf{x} - \mathbf{x}_1)]\} * \mathcal{F}\{\exp[i\varphi_2(\mathbf{x} - \mathbf{x}_2)]\} * \ldots. \end{aligned} \quad (2)$$

This expression involves many operations of convolution, denoted by $*$, which are not easy to calculate. Numerically, diffracted-beam amplitudes are never evaluated using this expression. In the limiting case of zero crystal thickness or scattering power, we may assume that the condition

$$\sum_n \varphi_n(\mathbf{x} - \mathbf{x}_n) \ll 1$$

is satisfied by all atoms involved such that a *weak-phase-object approximation* (WPOA) becomes valid and the expression for the diffracted-beam amplitude (2) reduces to

$$\begin{aligned} A(\mathbf{q}) &= \mathcal{F}\left\{\exp\left[i \sum_n \varphi_n(\mathbf{x} - \mathbf{x}_n)\right]\right\} \\ &\approx \mathcal{F}\left\{1 + i \sum_n \varphi_n(\mathbf{x} - \mathbf{x}_n)\right\} \\ &= \delta(\mathbf{q}) + i \sum_n f_n(s) \exp(2\pi i \mathbf{q} \cdot \mathbf{x}_n), \end{aligned} \quad (3)$$

and this is the kinematic expression for the diffracted-beam amplitudes by a projected potential. In general, this expression is invalid quantitatively even for a single layer of atoms, and consequently the structural refinement procedure cannot be based on this expression.

Formally, we may define a dynamical scattering factor

$$f^{(d)}(\mathbf{q}) = -i\mathcal{F}\{\exp[i\varphi(\mathbf{x})] - 1\}, \quad (4)$$

so that for a single atom we have

$$A(\mathbf{q}) = \mathcal{F}\{\exp[i\varphi(\mathbf{x})]\} = \delta(\mathbf{q}) + if^{(d)}(\mathbf{q}). \quad (5)$$

This is very similar to what Cowley & Moodie did in their 1959 paper on the scattering of electrons by atoms and crystals. The Cowley & Moodie phase atom, *i.e.* an atom represented in the form $\exp[i\varphi(\mathbf{x})]$, may be derived from a more accurate Molière high-energy approximation (Molière, 1947) derived from the general partial wave theory of scattering from a central force field (see also Glauber, 1959) by making a small-angle approximation. Detailed calculation shows that the Molière high-energy approximation agrees with the exact partial-wave method to an accuracy of 1% up to scattering angles of 10° (Zeitler, 1964, 1967) and that the Cowley & Moodie phase-atom approximation agrees with the more accurate methods for most atoms over the range of scattering angles normally used in diffraction experiments with solids (Cowley, 1990).

It should be pointed out that $f^{(d)}(\mathbf{q})$ defined above in (4) is an atomic quantity, meaning that it is independent of the environment in which the atom is embedded. This factor depends, however, on the acceleration voltage *E*. Numerically, $f^{(d)}(\mathbf{q})$ may be readily obtained by using an analytical expression for the Cowley & Moodie phase atom $\exp[i\varphi(\mathbf{x})]$ [see equation (5)] and one of the FFT routines [*e.g.* routine *FOURN.f* given in *Numerical Recipes* (Press *et al.*, 1986)]. In equation (5), the first term corresponds to the incident plane wave along the *z* axis and the second term to the diffracted wave. In general, the factor $f^{(d)}(\mathbf{q})$ is a complex quantity as shown in Fig. 1 for platinum and oxygen atoms. If we further assume that we may neglect higher-order terms, equation (2) then becomes
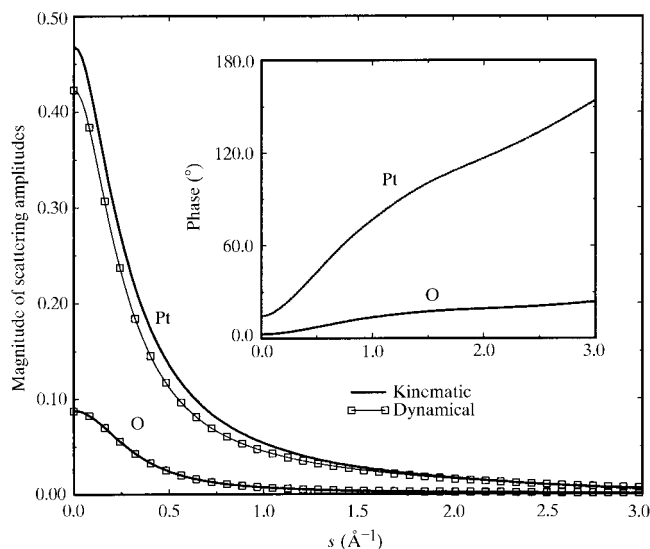
Figure 1
The magnitudes and phases of the electron scattering amplitudes for Pt and O atoms. The primary-beam energy is 100 keV.

$$A(\mathbf{q}) = \mathcal{F}\{\exp[i\varphi_1(\mathbf{x} - \mathbf{x}_1)]\} * \mathcal{F}\{\exp[i\varphi_2(\mathbf{x} - \mathbf{x}_2)]\} * \ldots$$
$$= \{\delta(\mathbf{q}) + if_1^{(d)}(\mathbf{q})\exp(2\pi i\mathbf{q} \cdot \mathbf{x}_1)\}$$
$$* \{\delta(\mathbf{q}) + if_2^{(d)}(\mathbf{q})\exp(2\pi i\mathbf{q} \cdot \mathbf{x}_2)\} * \ldots$$
$$\approx \delta(\mathbf{q}) + i\sum_n f_n^{(d)}(\mathbf{q})\exp(2\pi i\mathbf{q} \cdot \mathbf{x}_n), \tag{6}$$

i.e. the dynamical diffracted-beam amplitudes are proportional to the *dynamical structure factors* of the crystal,

$$F^{(d)}(s) = \sum_n f_n^{(d)}(\mathbf{q})\exp(2\pi i\mathbf{q} \cdot \mathbf{x}_n).$$

This expression is identical to the kinematic expression (3), but with the electron atomic scattering factors f_n being replaced by the dynamical scattering factor $f_n^{(d)}$, and the error introduced in this approximation is of the second order in $|f^{(d)}(s)|$, *i.e.* $\mathcal{O}[(f_n^{(d)})^2]$. Explicitly, the leading terms of the error function $\mathcal{O}[(f_n^{(d)})^2]$ for all $\mathbf{q} \neq 0$ are given by

$$\mathcal{O}[(f_n^{(d)})^2] = \sum_{j,k<j}[if_j^{(d)}(\mathbf{q})\exp(2\pi i\mathbf{q} \cdot \mathbf{x}_j)]$$
$$* [if_k^{(d)}(\mathbf{q})\exp(2\pi i\mathbf{q} \cdot \mathbf{x}_k)]$$
$$+ \sum_{j,k<j,l<k}[if_j^{(d)}(\mathbf{q})\exp(2\pi i\mathbf{q} \cdot \mathbf{x}_j)]$$
$$* [if_k^{(d)}(\mathbf{q})\exp(2\pi i\mathbf{q} \cdot \mathbf{x}_k)]$$
$$* [if_l^{(d)}(\mathbf{q})\exp(2\pi i\mathbf{q} \cdot \mathbf{x}_l)] + \ldots$$
$$= \mathcal{F}\left\{\sum_{j,k<j}\varphi'(\mathbf{x} - \mathbf{x}_j)\varphi'(\mathbf{x} - \mathbf{x}_k)\right\}$$
$$+ \mathcal{F}\left\{\sum_{j,k<j,l<k}\varphi'(\mathbf{x} - \mathbf{x}_j)\varphi'(\mathbf{x} - \mathbf{x}_k)\varphi'(\mathbf{x} - \mathbf{x}_l)\right\}$$
$$+ \ldots, \tag{7}$$

where $\varphi'(\mathbf{x})$ is related to the inverse Fourier transform of the dynamical scattering factor $f^{(d)}(\mathbf{q})$. The error function $\mathcal{O}[(f_n^{(d)})^2]$ will have vanishing value when all atoms are well separated such that the overlap between different atoms are negligible, *i.e.* for all $j \neq k$ we have $\varphi'(\mathbf{x} - \mathbf{x}_j)\varphi'(\mathbf{x} - \mathbf{x}_k) \approx 0$. This requirement may be satisfied for a monolayer of a crystal and along a low-index zone axis where all atoms are laterally well separated and have different coordinates $\mathbf{x}_n$. Shown in Fig. 2(*a*) is a two-dimensional distribution of the [001] projected potential $\phi(x, y)$ for a monolayer of a GaAs single crystal. This figure shows four conventional GaAs unit cells, with a Ga atom sitting at the center of the figure, surrounded by 4 nearest As atoms, 8 second-nearest As atoms, 12 third-nearest Ga atoms and then 16 As atoms at the edges of the figures. All atoms are well separated in this case and there exists little overlap between neighboring atoms. Equation (6) is expected to work well in this case.

A thin film usually consists of more than a monolayer of a crystal. When high-energy electrons are incident at the thin film along a low-index zone axis, there exist many atom strings or columns of atoms each with common lateral atomic coordinates $\mathbf{x}_n$. Although overlap between different atom strings is small, overlap between atoms in the same string is large and cannot therefore be neglected. For a thin film consisting of

only a few monolayers of light atoms, we may neglect terms involving $[\varphi'(\mathbf{x})]^2$, *i.e.* assume that an electron will be scattered by each atom only once. In reciprocal space, this is equivalent to say that the validity of the kinematic type of expression (6) depends on the smallness of the magnitude of the dynamical scattering factor and, in general, the smaller the magnitude of $|f^{(d)}(s)|$ the better expression (6) works.

(a)

(b)
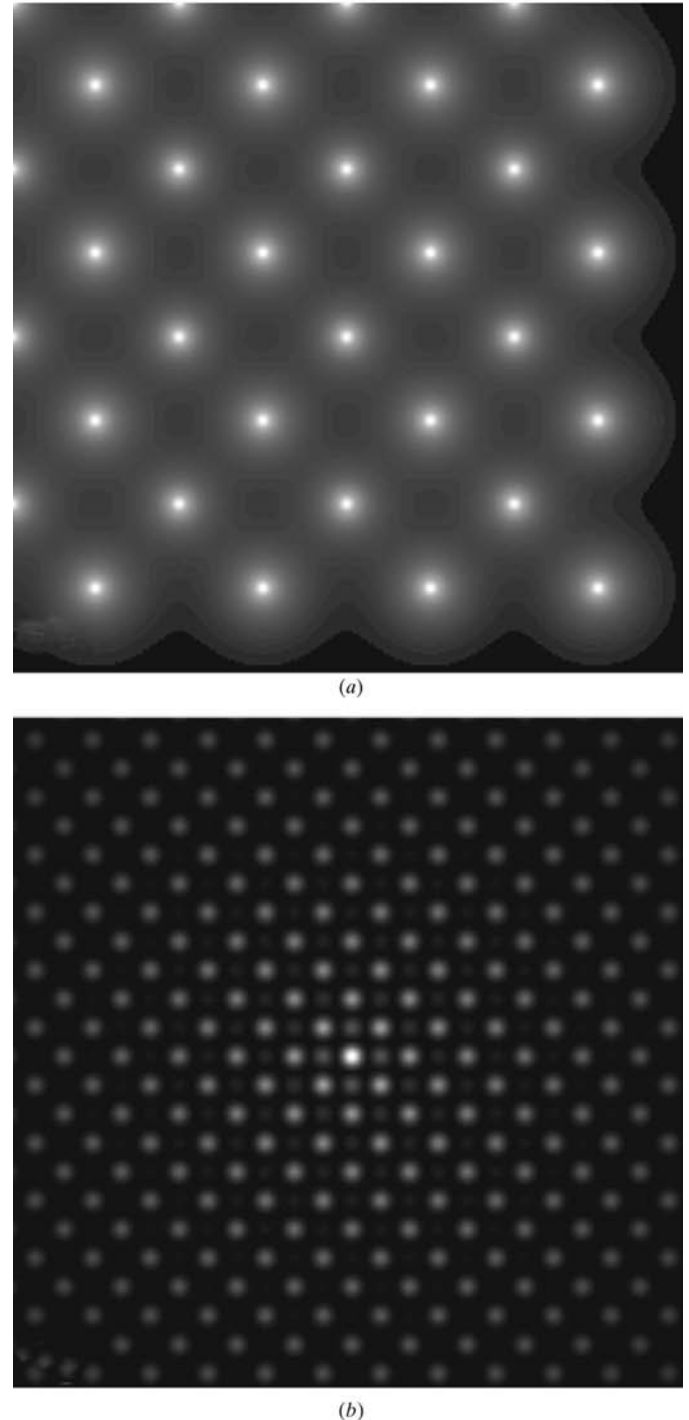
Figure 2
(*a*) Projected potential distribution for a GaAs single crystal and (*b*) corresponding electron diffraction pattern. The crystal thickness is 5.65 Å, the primary-beam energy is 100 keV and the incident-beam direction is along the [001] zone axis.

We now consider how to estimate the magnitude of dynamical scatterng factors. Utilizing the parameterized form of the electron atomic scattering factor (Peng, 1999; Doyle & Turner, 1968)

$$f(s) = \sum_k a_k \exp(-b_k s^2), \qquad (8)$$

we have the following expression for the three-dimensional distribution of the electrostatic potential of a single atom (Peng, 1999):

$$\phi(r) = \frac{h^2}{2\pi m_0 e} \sum_k a_k \left(\frac{4\pi}{b_k}\right)^{3/2} \exp\left[-\frac{4\pi^2}{b_k}(x^2 + y^2 + z^2)\right].$$
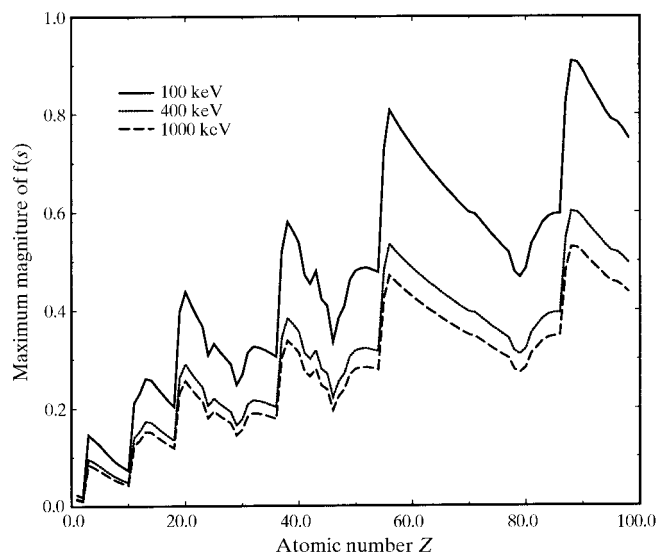
The projected potential is then given by

$$\phi(x, y) = \int_{-\infty}^{\infty} \phi(x, y, z)\, dz$$
$$= \frac{2h^2}{m_0 e} \sum_k \left(\frac{a_k}{b_k}\right) \exp\left[-\frac{4\pi^2}{b_k}(x^2 + y^2)\right].$$

For a single atom, we have the following expression for the exit electron wave function

$$\psi(x, y) = \exp\left\{ i4\pi\lambda\left(1 + \frac{eE}{m_0 c^2}\right) \sum_k \left(\frac{a_k}{b_k}\right)\right.$$
$$\left. \times \exp\left[-\frac{4\pi^2}{b_k}(x^2 + y^2)\right]\right\}, \qquad (9)$$

and numerically the dynamical scattering factor may be readily obtained by Fourier transform of this function. Shown in Fig. 3 are maximum magnitudes of the dynamical scattering factors (occurring at zero angle of scattering) for all neutron atoms in the Periodic Table and three accelerating voltages. It is seen that for all atoms we have $f_{max}^{(d)} < 1.0$, and the magnitudes decrease substantially from that at 100 to 400 keV.

An estimation of the magnitudes may be made using the WPOA. Using (9), the WPOA diffracted-beam amplitude is given by
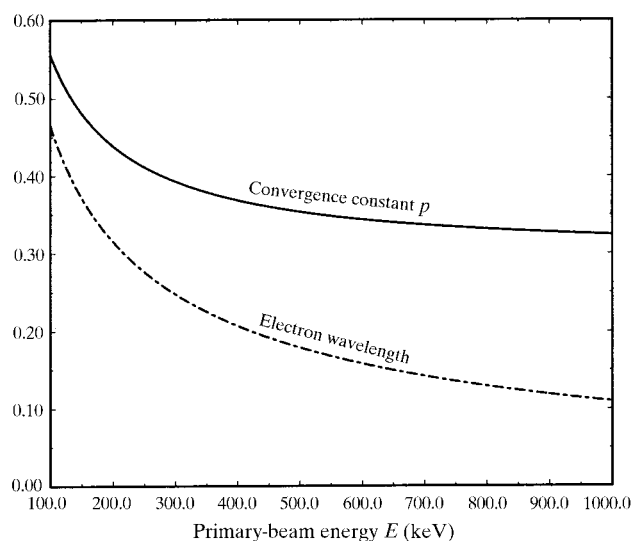
$$f(q_x, q_y) = -i\mathcal{F}\{\psi(x, y) - 1\}$$
$$= \mathcal{F}\left\{ 4\pi\lambda\left(1 + \frac{eE}{m_0 c^2}\right) \sum_k \frac{a_k}{b_k} \exp\left[-\frac{4\pi^2}{b_k}(x^2 + y^2)\right]\right\}$$
$$= \lambda\left(1 + \frac{eE}{m_0 c^2}\right) \sum_k a_k \exp\left[-\frac{b_k}{(4\pi)^2}(q_x^2 + q_y^2)\right]. \quad (10)$$

Although the above expression differs substantially from the dynamical scattering factor, with the latter being in general a complex function, we note that even for a heavy atom such as a platinum atom the magnitude of the dynamical scattering factor differs only a few percent from the usual electron atomic scattering factor (see Fig. 1), we may therefore use the above formula (10) and a_k and b_k given by Peng (1999) to estimate the magnitude, noting that numerically the electron wavelength in the above expression is measured in Å, the primary-beam energy eE is measured in keV and that $m_0 c^2 = 511$ keV. Equation (10) shows clearly that the magnitude of the scattering amplitude $f(\mathbf{q})$ depends on the primary-beam energy *via* a parameter

$$p = \lambda(1 + eE/m_0 c^2) = h/m_0 \upsilon,$$

where υ is the velocity of the high-energy electron. This parameter decreases with increasing accelarating voltage E and approaches the Compton wavelength $\lambda_c = h/m_0 c$ and the dependence of the parameter on E is given in Fig. 4.

Taking silicon as an example, we have $a_1 = 0.3626$, $a_2 = 0.9737$, $a_3 = 2.7209$, $a_4 = 1.7660$ Å, $\lambda = 0.037$ and 0.0164 Å for 100 and 400 keV, respectively. It can be easily estimated that for 100 keV the higher-order terms will become comparable to that appearing in equation (6) for about four monolayers of silicon crystal; for 400 keV, the number is about

Figure 3
Maximum magnitudes of dynamical scattering amplitudes for all neutral atoms in the Periodic Table and three different voltages.

Figure 4
Voltage dependence of the parameter p and the wavelength of the incident electron. Both p and λ are given in Å.

six. On the other hand, for La, these numbers are reduced by three times, *i.e.* are of the order of a monolayer. Equation (6) is therefore not valid in general for thin films composed of more than a monolayer of heavy atoms.

We now consider an alternative expression to (6). Assuming that there exists ℓ_n atoms in the nth atom string, the exit electron wave function $\psi(\mathbf{x})$ may then be written as

$$\psi(\mathbf{x}) = \exp\left\{i\sum_n \ell_n\varphi_n(\mathbf{x}-\mathbf{x}_n)\right\}.$$

In analogy with the definition of the dynamical scattering factor $f^{(d)}$, we may introduce a dynamical string scattering factor $f^{(s)}$ such that

$$f^{(s)}(s) = -i\mathcal{F}\{\exp[i\ell\varphi(\mathbf{x})]-1\}. \tag{11}$$

In terms of these dynamical string scattering factor, we may re-write (6) as

$$A(\mathbf{q}) = \delta(\mathbf{q}) + i\sum_n f^{(s)}(s)\exp(2\pi i\mathbf{q}\cdot\mathbf{x}_n), \tag{12}$$

and again a kinematic type of expression is obtained.

3. Results and discussion

Fig. 2(*b*) shows a calculated [001] zone-axis electron diffraction pattern from a monolayer of a GaAs single crystal. The pattern corresponds to the projected potential shown in Fig. 2(*a*) and a primary-beam energy of 100 keV. In Fig. 2(*b*), the central bright spot is the transmitted zero spot, the surrounding four weak spots are (200), (020), ($\bar{2}$00) and (0$\bar{2}$0). The horizontal line passing through the zero beam therefore contains visible (200), (400), (800), (12,0,0) (16,0,0) and (20,0,0) reflections toward the right of the zero beam.

Shown in Fig. 5 are the calculated (*a*) magnitudes and (*b*) phases of reflections lying on the horizontal line passing through the zero spot shown in the center of Fig. 2(*b*). The three curves shown in the figure were calculated using full dynamical theory, kinematic type of dynamical electron diffraction theory, *i.e.* equation (6), and kinematic theory, respectively. It is seen that although the kinematic theory results in roughly correct magnitudes of the diffracted beams (Fig. 5*a*) for a monolayer of a GaAs crystal, it fails completely in predicting the dependence of the phases of the diffracted beams on the angles of scattering. The quasi-dynamical expression (6), on the other hand, reproduces beautifully both the magnitudes and phases for all beams.

Another interesting feature shown in Fig. 5 is that although the phases of the diffracted-beam amplitudes as predicted by the kinematic theory are completely wrong, especially for higher-order reflections, the magnitudes predicted by the kinematic theory agree well with that predicted by the full dynamical theory. Within the validity of (6), we will show that this can be proved analytically for crystals composed of only one kind of atom. By writing the dynamical scattering factor

as $f^{(d)}(\mathbf{q}) = f(\mathbf{q})\exp[i\theta(\mathbf{q})]$ and using (6), we obtain the diffracted-beam intensities

$$\begin{aligned}
I(\mathbf{q}) &= A(\mathbf{q})\cdot A^*(\mathbf{q}) \\
&= \left\{\delta(\mathbf{q}) + i\sum_n f_n(\mathbf{q})\exp[i\theta_n(\mathbf{q})]\exp[2\pi i\mathbf{q}\cdot\mathbf{x}_n]\right\} \\
&\quad \times \left\{\delta(\mathbf{q}) - i\sum_n f_n(\mathbf{q})\exp[-i\theta_n(\mathbf{q})]\exp[-2\pi i\mathbf{q}\cdot\mathbf{x}_n]\right\} \\
&= \delta(\mathbf{q}) - 2\sum_n f_n(0)\sin\theta_n(0) + \sum_{n\neq n'} f_n(\mathbf{q})f_{n'}(\mathbf{q}) \\
&\quad \times \exp\{i[\theta_n(\mathbf{q})-\theta_{n'}(\mathbf{q})]\}\exp[2\pi i\mathbf{q}\cdot(\mathbf{x}_n-\mathbf{x}_{n'})].
\end{aligned}$$

For a crystal with only one kind of atom and non-zero angle of scattering, we have

$$I(\mathbf{q}) = \left|\sum_n f_n(\mathbf{q})\exp(2\pi i\mathbf{q}\cdot\mathbf{x}_n)\right|^2, \tag{13}$$

that is the diffracted-beam intensities are exactly the same as that from a crystal as if it was composed of atoms all with zero
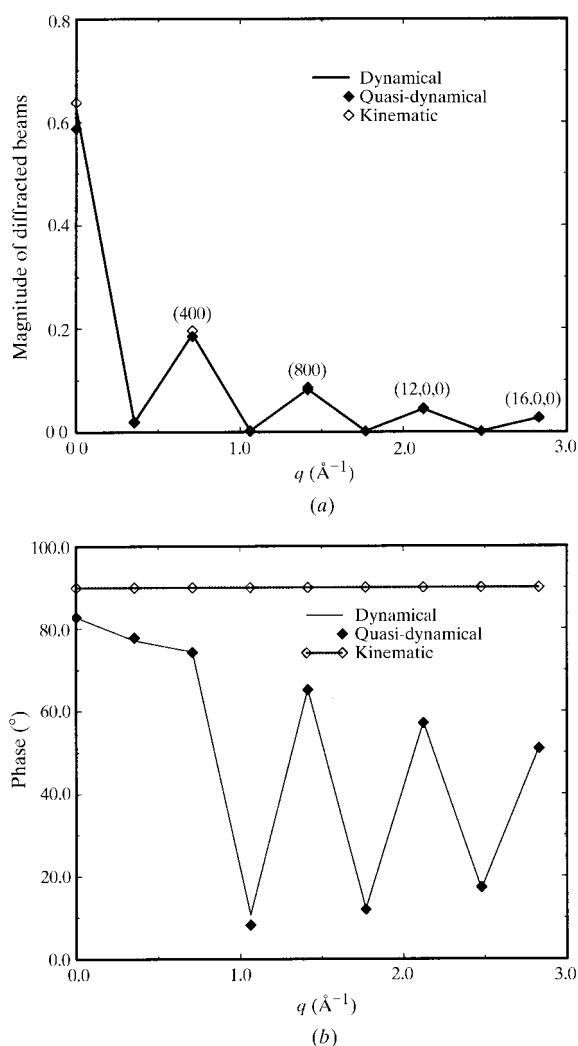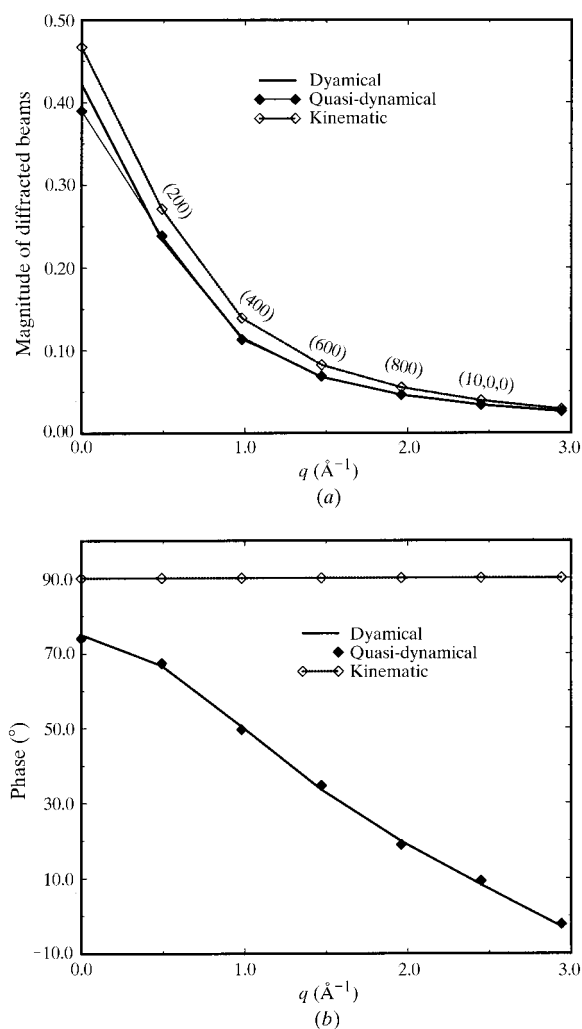

Figure 5
Calculated (*a*) magnitudes and (*b*) phases of several diffracted beams from a GaAs single crystal. These diffracted beams correspond to (200), (400), (600), (800), (10,0,0), (12,0,0) and (16,0,0) reflections, respectively.

phases $\theta_n(\mathbf{q}) = 0$. For light atoms, such as H and O, and moderately heavy atoms, such as Ga and As, the kinematic and dynamical scattering factors have almost the same magnitude $|f(\mathbf{q})|$ as the dynamical scattering factor; equation (13) shows that the kinematic theory and therefore the usual electron atomic scattering factors may be used for constructing potential maps $V(\mathbf{x})$ and in structural refinement.

For heavy atoms, such as Pt and Au, the magnitude of the dynamical scattering factor differs by a few percent from that of the usual atomic scattering factor (see Fig. 1). The kinematic theory is expected to work reasonably well but be quantitatively not accurate. Shown in Fig. 6 are calculated diffracted-beam magnitudes and phases from a monolayer of Au atoms. The three curves shown in the figure were calculated using the full dynamical theory, the kinematic theory and the quasi-dynamical expression (6). This figure shows clearly that, for even a monolayer of Au atoms, the diffracted-beam magnitudes start to deviate from the kinematic theory, unlike that for crystals composed of only light and moderately heavy

atoms, and that the kinematic phases are very different from the true dynamical phases. The quasi-dynamical expression (6), on the other hand, again reproduced excellently both the magnitudes and phases of these diffracted-beam amplitudes except the zero beam. The error in the zero beam is due mainly to the fact that to a first-order approximation the overlap between adjacent atoms may be taken into account *via* a shift in the crystal inner potential (Peng *et al.*, 1998), or in other words the overlap affects mainly the zero and lowest-order reflections.

We now consider diffraction by a thin film composed of heavy scatters, that is a film composed of 40 layers of Au atoms. Application of the quasi-dyanmical expression (6) fails to predict correctly both the phases and magnitudes for this thin film, as shown clearly in Fig. 7. The three curves shown in the figure were calculated for 100 keV using full dynamical theory (denoted as dynamical), direct summation of dynamical atomic scattering factors (denoted as atomic factor)

Figure 6
Calculated (*a*) magnitudes and (*b*) phases of several diffracted beams from a monolayer of a single crystal of Au. These diffracted beams correspond to the (200), (400), (600), (800), (10,0,0) and (12,0,0) reflections, respectively.
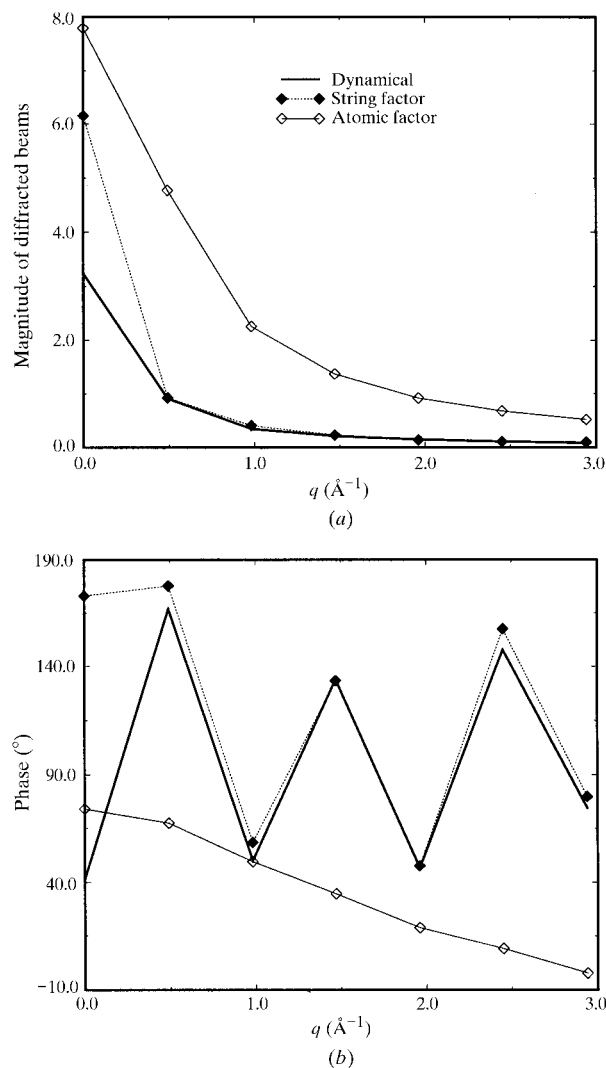
Figure 7
Calculated (*a*) magnitudes and (*b*) phases of diffracted-beam amplitudes from a thin film composed of 40 layers of Au atoms and for a primary-beam energy of 100 keV.

and summation over dynamical string scattering factors (denoted as string factor). These figures show that, for scattering by a film composed of even heavy scatters like Au, the kinematic type of expression (12) for atom strings works well. In crystal structural refinement, only two parameters are needed for each atom string, that is the atomic species and number of atoms within each string. The task of structural refinement based on expression (12) is expected to be much easier than a full refinement based on the full dynamical diffraction theory (Tsuda & Tanaka, 1995).

For a thin film composed of a single layer of Au atoms, Fig. 6 shows that the phase of the diffracted electron beam decreases with increasing angle of scattering. For a thicker film composed of 40 layers of Au atoms (see Fig. 7), however, the phase shows an oscillating dependence on the angle of scattering. This oscillating behavior may be understood from the POA expression for the exit electron wave function

$$\psi(\mathbf{x}) = \exp[i\Phi(\mathbf{x})] = \cos[\Phi(\mathbf{x})] + i\sin[\Phi(\mathbf{x})],$$

where

$$\Phi(\mathbf{x}) = \sum_n \varphi_n(\mathbf{x} - \mathbf{x}_n)$$

is the total projected potential of the thin film. For a very thin film, we have

$$\psi(\mathbf{x}) \approx 1 + i\Phi(\mathbf{x}),$$

i.e. the imaginary part of the electron wave function is proportional to the projected potential. Shown in Fig. 8 are calculated imaginary parts of the electron wave function for a thin film of Au. The three curves shown in the figure were calculated for an Au film of 0.2 monolayer, 0.7 monolayer and 2.5 monolayer, respectively. The curve marked 0.2 monolayer represents roughly the projected potential distribution, and corresponding variation in the phases of the diffracted beams with scattering angle are determined mainly by the structure of the crystal.
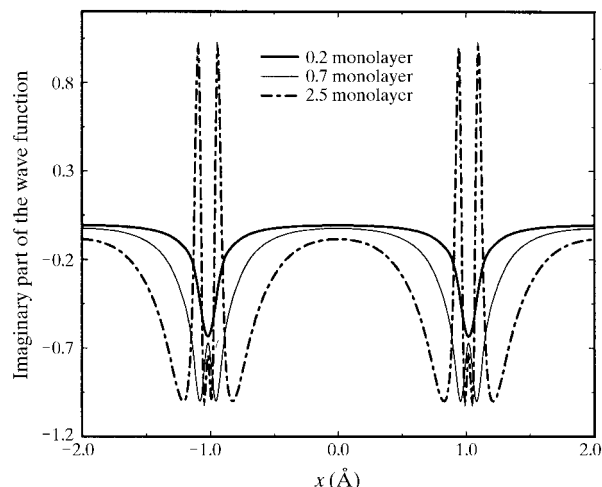
Figure 8
Calculated imaginary part of the electron wave function after passing through a thin film of Au.

For a slightly thicker film satisfying the condition

$$\{\Phi(\mathbf{x})\}_{max} < \pi/2,$$

where the subscript max denotes the maximum value of the projected potential, the imaginary part of the electron wave function does not have a simple linear relation with the projected potential. Nevertheless, the imaginary part of the wave function shows a singly peaked distribution around each atomic site, and Fourier transform of this part gives a distribution that decreases with increasing scattering angle and a phase variation as shown in Fig. 7 (curve marked with atomic factor).

For a thicker film with

$$\{\Phi(\mathbf{x})\}_{max} > \pi/2,$$

multiple peaked distribution is expected around each atomic site for the imaginary part of the electron wave function. The curve shown in Fig. 8 and marked 0.7 monolayer was calculated for an Au film of 0.7 monolayer thick. This film has a maximum value of the projected potential $\{\Phi(\mathbf{x})\}_{max}$ that is slightly larger than $\pi/2$. The imaginary part of the electron wave function is seen to have split into a two-peaked distribution around each atomic site. With increasing film thickness, more oscillations are introduced around the atomic sites (see Fig. 8, the curve marked 2.5 monolayer). Fourier transform of this oscillating imaginary part of the electron wave function will also exhibit oscillations, leading to oscillating phases of the diffracted electron beams.

Approximating the projected potential around each atom with an ideal potential well of constant depth, i.e.

$$\Phi(\mathbf{x}) = \begin{cases} V_0 t, & \text{if inside the potential well} \\ 0 & \text{otherwise}, \end{cases}$$

where t is the thickness of the film. The electron wave function will then become a periodic function of t, its periodicity being $2\pi/V_0$. Although this ideal situation cannot be realized in practice, a tightly bound Bloch wave excited in the crystal feels a constant potential (Peng & Gjønnes, 1989) very similar to the ideal situation described above. For each strongly excited Bloch wave, we then expect a periodicity in its thickness dependence. When two or more Bloch waves are strongly excited, more than one periodicity is involved and interference between different Bloch waves will result in complicated contrast with varying crystal thickness, i.e. thickness fringes.

4. Conclusions

In this paper, we have shown that, for a thin film, when there exists little or negligible overlap between electrostatic potentials of adjacent atoms, the dynamical diffracted-beam amplitudes may be expressed as a summation of dynamical scattering factors

$$A(\mathbf{q}) = \delta(\mathbf{q}) + i\sum_n f_n^{(d)}(s)\exp(2\pi i\mathbf{q}\cdot\mathbf{x}_n), \qquad (14)$$

that is a kinematic type of expression for the dynamical diffracted-beam amplitudes is obtained. For light and

moderately heavy atoms, the dynamical atomic scattering factor $f^{(d)}(s)$ has almost identical magnitude to the usual electron atomic scattering factor, such as those tabulated by Peng et al. (Peng et al., 1996; Peng, 1999). For heavy atoms, the magnitude of $f^{(d)}(s)$ may differ from the usual electron atomic scattering factor by a few percent.

We have shown that, for thin crystals composed of only light and moderately heavy atoms, the phases of the diffracted electron-beam amplitudes may differ substantially from that predicted by the kinematic theory. The diffracted-beam intensities are, however, identical to those resulting from a crystal as if it was composed of atoms all having zero phases [i.e. as if $f^{(d)}(s)$ was real]. For crystals composed of heavy atoms, the above statement remains valid but the real scattering factors $f^{(d)}(s)$ differ by a few percent from the usual atomic scattering factors. The kinematic theory is expected to work reasonably well but not be quantitatively accurate.

For a moderately thicker crystal when the kinematic type of expression (14) based on dynamical scattering factors are not valid but the phase-object approximation is still a good one, a similar kinematic type of expression may be obtained where the dynamical atomic scattering factors are replaced by dynamical string scattering factors $f^{(s)}(s)$. This new expression is slightly more complicated than cases when there exists negligible overlap between adjacent atoms, for two parameters are now required to specify an atom string, i.e. the atomic species and number of atoms in the string, but it reproduces well both the phases and magnitudes of the diffracted electron-beam amplitudes.

For thicker crystals, the phase-object approximation becomes less accurate and our kinematic type of expressions cannot be applied quantitatively for analyzing experimental microscopy data. Extensive computation reveals, however, that the atom string approximation works well even for crystals with larger thickness. This fact suggests that a kinematic type of approximation works even for crystals with thicknesses much larger than 100 Å. The effective scattering factors involved in the expression cannot, however, be simply related to the atomic or string potential. For moderate accelerating voltages, Van Dyck & Op de Beeck (1996) have shown that the diffracted-beam amplitudes may be related to some bound eigenstates of the projected atom string potentials. These string potentials depend, however, on the interatomic distances along the strings and therefore are not true atomic quantities. It has been shown nevertheless that the kinematic types of expression are useful in many important applications, including calculating high-resolution electron images, diffuse scattering and structure retrieval.

In a previous publication (Peng & Wang, 1994), we have shown that the kinematic theory works better for lower angles of scattering. The argument behind that conclusion is that electrons are most likely to suffer from multiple-scattering events if the electrons are incident at the atoms with smaller impact distances (i.e. the nearest electron–nucleus distance) and therefore being scattered toward larger angles. In the light of the present work, our earlier conclusion simply means that

the dynamical scattering factors may be approximated by the kinematic atomic scattering factors better for lower-order reflections than for higher-order reflections. The argument presented in the present work is therefore more general and may be used even quantitatively for analyzing electron microscopy data from a thin film.

References

Cowley, J. M. (1990). *Diffraction Physics*, 2nd ed. Amsterdam: North-Holland.
Cowley, J. M. (1992). In *International Tables for Crystallography*, Volume C, edited by A. J. C. Wilson. Dordrecht/Boston/London: Kluwer Academic Publishers.
Cowley, J. & Moodie, A. (1957). *Acta Cryst.* **10**, 609–619.
Cowley, J. & Moodie, A. (1959). *Acta Cryst.* **12**, 360–367.
Dorset, D. L. (1995). *Structural Electron Crystallography*. New York: Plenum Press.
Doyle, P. & Turner, P. (1968). *Acta Cryst.* A**24**, 390–397.
Gjønnes, J., Olsen, A. & Matsuhata, H. (1989). *J. Electron Microsc. Tech.* **13**, 98–110.
Glauber, R. (1959). *Lectures in Theoretical Physics*, edited by W. Brittin & G. Dunham, pp. 315–372. New York: Interscience.
Glauber, R. & Schomaker, V. (1953). *Phys. Rev.* **89**, 667–671.
Goodman, P. & Moodie, A. (1974). *Acta Cryst.* A**30**, 280–290.
Hirsch, P. B., Howie, A., Nicholson, R., Pashley, D. & Whelan, M. (1977). *Electron Microscopy of Thin Crystals*. Malabar/Florida: Krieger Publishing Company.
Hoerni, J. & Ibers, J. (1953). *Phys. Rev.* **91**, 1182–1185.
Humphreys, C. J. (1979). *Rep. Prog. Phys.* **42**, 1825–1887.
Ibers, J. & Hoerni, J. (1954). *Acta Cryst.* **7**, 405–408.
Li, F. & Tang, D. (1985). *Acta Cryst.* A**41**, 376–382.
Marks, L. & Landree, E. (1998). *Acta Cryst.* A**54**, 296–305.
Molière, G. (1947). *Z. Naturforsch. Teil A*, **2**, 133–157.
Peng, L.-M. (1999). *Micron*, **30**, 625–649.
Peng, L.-M., Dudarev, S. & Whelan, M. (1998). *Phys. Rev. B*, **57**, 7259–7265.
Peng, L.-M. & Gjønnes, J. K. (1989). *Acta Cryst.* A**45**, 699–703.
Peng, L.-M., Ren, G., Dudarev, S. & Whelan, M. (1996). *Acta Cryst.* A**52**, 257–276.
Peng, L.-M. & Wang, S. (1994). *Acta Cryst.* A**50**, 759–771.
Press, W. H., Flannery, B. P., Teukolsky, S. & Vetterling, W. (1986). *Numerical Recipes*. Cambridge University Press.
Ren, G., Zuo, J. M. & Peng, L.-M. (1997). *Micron*, **28**, 459–467.
Spence, J. (1993). *Acta Cryst.* A**49**, 231–260.
Spence, J. & Zuo, J. (1992). *Electron Microdiffraction*. New York/London: Plenum Press.
Tivol, W. (1999). Editor. *Microscopy Research and Technology*, Vol. 46, No. 2/3.
Tsuda, K. & Tanaka, M. (1995). *Acta Cryst.* A**51**, 7–19.
Van Dyck, D. & Op de Beeck, M. (1996). *Ultramicroscopy*, **64**, 99–107.
Vincent, R., Bird, D. & Steeds, J. W. (1984). *Philos. Mag. A*, **50**, 765–786.
Woolfson, M. & Fan, H. F. (1995). *Physical and Non-physical Methods of Solving Crystal Structures*. Cambridge University Press.
Zeitler, E. (1964). *Phys. Rev.* **136**, A1546–A1552.
Zeitler, E. (1967). *Phys. Rev. B*, **162**, 1439–1447.